VILNIUS UNIVERSITY

CENTER FOR PHYSICAL SCIENCES AND TECHNOLOGY

Gediminas Braziulis

SYNTHESIS AND INVESTIGATION OF ALKALINE EARHT METAL MOLYBDATES

Summary of doctoral dissertation

Physical Sciences, Chemistry (03 P)

Vilnius, 2017

The dissertation was carried out from 2013 to 2017 at Vilnius University.

Scientific supervisor:

Assoc. Prof. Dr. Artūras Žalga (Vilnius University, Physical Sciences, Chemistry – 03 P).

Evaluation board:

Chairman:

Prof. Habil. Dr. Rimantas Ramanauskas (Center for Physical Sciences and Technology, Physical Sciences, Chemistry – 03 P).

Members:

Prof. Dr. Eugenijus Valatka (Kaunas University of Technology, Technological Sciences, Chemical Engineering 05T).

Prof. Dr. Jūratė Senvaitienė (Vilnius University, Physical Sciences, Chemistry – 03 P).

Dr. Živilė Stankevičiūtė (Vilnius University, Physical Sciences, Chemistry – 03 P).

Dr. Anatoli Popov (University of Latvia, Physical Sciences, Physics – 02P).

The official discussion will be held on 2 p.m. on the 22th of December 2017, at the meeting of the Evaluation Board at the Auditorium of Inorganic Chemistry of the Faculty of Chemistry of Vilnius University.

Address: Naugarduko 24, LT-03225 Vilnius, Lithuania. Tel. 2193108. Fax: 2330987.

The summary of doctoral dissertation was mailed on the 20th of November 2017.

The dissertation is available at the Library of Vilnius University, Library of Center for Physical Sciences and Technology and online:

www.vu.lt/lt/naujienos/ivykiukalendorius.

VILNIAUS UNIVERSITETAS

FIZINIŲ IR TECHNOLOGIJOS MOKSLŲ CENTRAS

Gediminas Braziulis

ŠARMINIŲ ŽEMIŲ METALŲ MOLIBDATŲ SINTEZĖ IR TYRIMAS

Daktaro disertacijos santrauka

Fiziniai mokslai, chemija (03 P)

Vilnius, 2017

3

Disertacija parengta 2013–2017 metais Vilniaus universitete.

Mokslinis vadovas:

        doc. dr. Artūras Žalga (Vilniaus universitetas, fiziniai mokslai, chemija – 03P).

Disertacija ginama viešame disertacijos gynimo tarybos posėdyje:

Pirmininkas:

        prof. habil. dr. Rimantas Ramanauskas (Fizinių ir technologijos mokslų centras, fiziniai mokslai, chemija – 03P).

Nariai:

        Prof. dr. Eugenijus Valatka (Kauno technologijos universitetas, technologijos mokslai, chemijos inžinerija 05T).

        Prof. dr. Jūratė Senvaitienė (Vilniaus universitetas, fiziniai mokslai, chemija – 03P).

        Dr. Živilė Stankevičiūtė (Vilniaus universitetas, fiziniai mokslai, chemija – 03P).

        Dr. Anatoli Popov (Latvijos universitetas, fiziniai mokslai, fizika – 02P).

Disertacija bus ginama viešame disertacijos gynimo tarybos posėdyje
2017 m. gruodžio mėn. 22 d. 14 val. Vilniaus universiteto Chemijos fakulteto Neorganinės chemijos auditorijoje.
Adresas: Naugarduko 24, LT-03225 Vilnius, Lietuva. Tel.: 2193108. Faksas: 2330987.
Disertacijos santrauka išsiuntinėta 2017 m. lapkričio mėn. 22 d.
Disertaciją galima peržiūrėti Vilniaus universiteto ir FTMC bibliotekose, bei VU interneto svetainėje adresu: www.vu.lt/lt/naujienos/ivykiu-kalendorius.

1. INTRODUCTION

Metal molybdates of the general formula $AMoO_4$ (A = Mg, Ca, Sr, Ba, Cd, Zn, Pb and etc.) have been studied extensively for decades, owing to their technological importance in a variety of applications such as phosphors [1-3], scintillation materials, microwave devices, catalysts or optoelectronic devices. From the structural point, the differences between alkaline earth metal molybdates ($AMoO_4$, A = Mg, Ca, Sr and Ba) mainly consist in ionic radius of the A-site. If the ionic radius of the A-site ion is smaller than 1.0 Å as is the case for $MgMoO_4$ ceramic, the compounds show a wolframite structure with octahedral coordination. Alternatively, if the ionic radius of the A-site is larger than 1.0 Å as is the case for Ca^{2+}, Sr^{2+} and Ba^{2+} in $AMoO_4$, the compounds show a scheelite structure with tetrahedral coordination. Moreover, as well as the crystal structure the surface morphology also significantly affects both the optical and electrical properties of alkaline earth metal molybdates. Thus, according to this the synthesis method that could be chosen for the preparation of these ceramic materials has significant importance.

In the last several decades, many different preparation techniques have been used for the preparation of $AMoO_4$ (A = Mg, Ca, Sr and Ba) ceramics. Nowadays, the results of obtained compounds, depending on the preparation route, are important and have significant influence to the science and technologies. Therefore, the choice of synthesis technique usually depends on variety factors that can shorten, facilitates and reduce the preparation way. From this point of view, the solution-based synthetic methods play a crucial role in the design and production of fine ceramics and they have been successful in overcoming many of the limitation of the traditional solid-state, high-temperature methods. The use of solution chemistry can eliminate major problems, such as long diffusion paths, impurities, and agglomeration, and result in products with improved homogeneity. Moreover, the sintering temperature that usually strong affects the properties of final compounds is crucial factor for the preparation of both nano-sized materials and thin films on different substrates.

The motivation of this dissertation thesis was to develop the aqueous sol-gel synthesis technique for the preparation of M'–Mo–O tartrate (M'=Mg, Ca, Sr and Ba) gel precursors and Powellite type $CaMoO_4:xEu^{3+}$ compounds in the sol-gel processing using tartaric acid as a complexing agent.

The main objective of this work was to synthesize alkaline earth metal molybdates and $CaMoO_4$:xEu^{3+} ceramics using aqueous tartaric acid-assisted sol-gel synthesis method and to investigate the thermal decomposition of as-prepared M'–Mo–O tartrate gel precursors taking in account the formation of the crystal structure of final ceramics, the peculiarities of their surface morphology, the characteristic vibrations of chemical bonds and optical properties of prepared compounds. For this reason, there were formulated tasks as follows:

1. To synthesize $MgMoO_4$, $CaMoO_4$, $SrMoO_4$, $BaMoO_4$, $CaMoO_4$:xEu^{3+} ceramics in the sol-gel processing using tartaric acid as a complexing agent.

2. To investigate the decomposition of as-prepared Mg–Mo–O, Ca–Mo–O, Sr–Mo–O and Ba–Mo–O gels using thermogravimetric (TG) and differential scanning calorimetric (DSC) analysis. Besides, to estimate the crystallization processes of the final $MgMoO_4$, $CaMoO_4$, $SrMoO_4$ and $BaMoO_4$ ceramics according to the TG-DSC analysis.

3. To determine the crystal phase composition of the obtained double oxides that were sintered at 500, 600, 700, 800, 900 ir 1,000 ^oC by the X-Ray diffraction analysis.

4. To compare the peculiarities of surface morphology of $MgMoO_4$, $CaMoO_4$, $SrMoO_4$, $BaMoO_4$, ir $CaMoO_4$:$x\%Eu^{3+}$ (x = 1, 2, 3, 4 ,5 ,6) compounds, which were annealed at different temperatures.

5. To characterize the FT–IR results of $CaMoO_4$:$x\%Eu^{3+}$ ceramics that was annealed at 650 ^oC.

6. To summarize the investigation of UV–Vis spectroscopy according to the amount of europium oxide in $CaMoO_4$ double oxide.

Statements of defense

1. For the first time the aqueous tartaric acid-assisted sol-gel synthesis technique was successfully proposed for the preparation of M'–Mo–O tartrate gels and $MgMoO_4$, $CaMoO_4$, $SrMoO_4$, $BaMoO_4$, ir $CaMoO_4$:$x\%Eu^{3+}$ ceramic materials.

2. It was demonstrated that TG–DSC analysis is powerful and suitable tool for both the investigation of decomposition mechanisms of Mg–Mo–O, Ca–Mo–O, Sr–Mo–O and Ba–Mo–O tartrate gel precursors and the estimation of the crystallization processes of the final $MgMoO_4$, $CaMoO_4$, $SrMoO_4$, and $BaMoO_4$ double oxides.

2. EXPERIMENTAL PART

The samples $MMoO_4$ (where M = Mg, Ca, Sr and Ba) and $CaMoO_4:xEu^{3+}$ with x=1, 2, 3, 4, 5 and 6 mol% of Eu^{3+} were prepared by an aqueous tartrate sol-gel synthesis route taking tartaric acid as a ligand. The magnesium (II) nitrate hexahydrate ($Mg(NO_3)_2 \cdot 6H_2O$, 99.97% AlfaAesar), calcium (II) nitrate tetrahydrate ($Ca(NO_3)_2 \cdot 4H_2O$, 99.98% AlfaAesar), strontium (II) nitrate ($Sr(NO_3)_2$, 99.97% AlfaAesar), barium (II) nitrate ($Ba(NO_3)_2$, 99.95% AlfaAesar), molybdenum oxide (MoO_3, 99.95% Alfa Aesar) and europium (III) oxide (Eu_2O_3, 99.99% AlfaAesar) were used as starting materials and weighed according to the desired stoichiometric ratio. Nitric acid (HNO_3), distilled water (H_2O) and ammonia ($NH_3 \cdot H_2O$) were used as solvents and reagents to regulate the pH of the solutions. Tartaric acid (TA, $C_4H_6O_6$, 99.5%) was used as a complexing agent. First, MoO_3 was dissolved in 25 ml of concentrated ammonia solution by stirring at 70–80 °C temperature. Then tartaric acid with a molar ratio of Mo / TA = 0.25, dissolved in a small amount of distilled water was added with a continuous stirring at the same temperature to the reaction mixture. Next, after several hours the stoichiometric amount of alkaline earth nitrate was mixed with the previous solution. To prevent precipitation the excess of ammonia was neutralized with concentrated HNO_3 until the pH reached the value of ~1.0. Finally, the same amount of the aqueous solution of the complexing agent TA was repeatedly added to the reaction mixture to prevent crystallization of metal salts during the gelation process. The beaker with the solution was closed with a watch glass and left for 1 h with continuous stirring. The obtained clear solution was concentrated by slow evaporation at 80 °C in an open beaker. A yellow transparent gel formed after nearly 90 % of the water has been evaporated under continuous stirring. After drying in an oven at 105 °C, fine-grained powders were obtained. The precursor gels were calcined for 5 h at 500 °C in alumina crucibles and reground carefully in an agate mortar. Since the gels are very combustible, slow heating (1 °C/min), especially between 150 and 300 °C, was found to be essential. After intermediate grinding the obtained powders were repeatedly annealed for 5 h at 500, 600, 700, 800, 900 and 1000 °C. Thermal measurements were performed with TG-DSC, STA 6000 Perkin-Elemer instrument using a sample weight of about 10 mg and a heating rate of 20 °C min^{-1} in flowing air (20 $cm^3 \cdot min^{-1}$) at ambient pressure from room temperature to 1000 °C. X-ray diffraction (XRD) patterns have been recorded

in air at room temperature with a powder X-ray diffractometer Rigaku MiniFlex II using CuKα$_1$ radiation. The spectra were recorded at the standard rate of 1.5 2θ/min. The scanning electron microscope (SEM) Hitachi TM3000 was used to study the surface morphology and microstructure of the obtained ceramic samples. The reflection spectra were recorded at room temperature using a Perkin Elmer Lambda 35 UV/VIS spectrometer. The samples were well glued up on the flat substrate in order to form thin layer on it and excited in 1100-200 nm wavelength interval.

3. RESULTS AND DISCUSSIONS

Thermal analysis

In order to explain the thermal decomposition behavior and crystallization processes of the synthesized M–Mo–O (M=Mg, Ca, Sr and Ba) tartrate gel precursors, the thermal analysis (TG/DSC) was performed. TG/DSC measurements of the alkaline earth metal molybdate tartrate gel precursors carried out up to 1000 °C at a heating rate of 20 °C/min in flowing air (20 cm^3/min) at ambient pressure with a sample weight of about 5 mg. The thermograms of analyzed samples are shown in Figs. 1 – 4, respectively.

At the initial stage of the explanation of TG curve, shown in Fig. 1, should be noted that the final weight loss of about 78 % occurred to 580 °C temperature, which gives the conclusion about the decomposition of all volatile organic parts in the gel precursor.
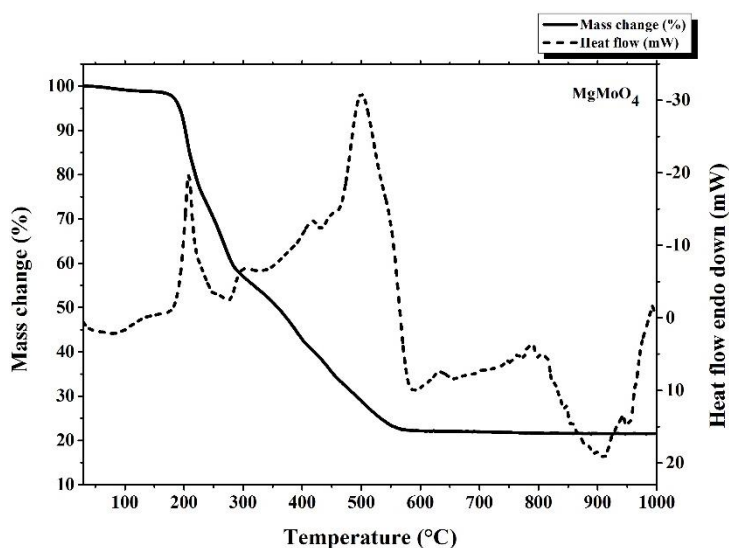

Fig. 1 Combined TG–DSC curves of the Mg–Mo–O tartrate gel precursor in flowing air

8

In general, the decomposition processes of the Mg–Mo–O tartrate system could be roughly divided into eight periods that clearly indicate all weight losses and heat flow transformations occurring during the sample heating in the appropriate range of temperature. The first weight loss of about 1 % in the TG curve goes from 40 ℃ to 140 ℃ temperatures and is related with the removal of surface absorbed water from the gel and/or water from the coordination sphere of the metal complexes. A broad endothermic peak with heat flow of 388 mJ and $\Delta H = 69,7$ J/g on the DSC curve corresponds to the first period of weight loss. By further increasing of temperature from 150 ℃ to 240 ℃ the weight of Mg–Mo–O tartrate precursor to 16,5 % has been decreased. A sharp exothermic peak of about 1280 mJ ($\Delta H = -230$ J/g) confirmed either by the initial decomposition of excess of tartaric acid in the precursor gel or by the decomposition reactions of mixed-metal nitrate and ammonium salts that formed during the sol–gel processing. The third weight loss (4.2 %) of precursor gel in 245 – 320 oC temperature range has been observed. The endothermic peak of about 510 mJ ($\Delta H = 92$ J/g) shows both the further decomposition of either tartaric acid or metal tartrates and the intermolecular rearrangement of organic compounds. Thereafter, on the following increasing of temperature fourth (2.7 %) and fifth (1 %) weight loss stages have started. Both small exothermic peaks of about 195 mJ ($\Delta H = -35$ J/g) and 22 mJ ($\Delta H = -4$ J/g) are attributed to the beginning of burning processes of residual organic compounds in the precursor gel. Finally, the last sixth weight loss of about 4 % from 470 ℃ to 580 ℃ temperature accords with the burning of elemental carbon in the residual sample. This process by strong exothermic peak of about 4920 mJ ($\Delta H = -882$ J/g) was confirmed, respectively. By further increasing of temperature, no weight losses in the TG curve have observed. Meanwhile, the results obtained from DSC measurement clearly indicated that at least two broad endothermic peaks 525 mJ ($\Delta H = 94$ J/g) and 6603 mJ ($\Delta H = 1185$ J/g) in the 600 – 1000 ℃ range of temperature have been related. Both of them came with the crystallization process of final structural materials. Moreover, according to the stabilized weight at temperatures higher than 800 ℃, no impurities phases either crystalline or amorphous have formed.

In conclusion, TG/DSC analysis of Mg–Mo–O tartrate gel precursor suggests that single-phase crystalline $MgMoO_4$ compound at relative low temperature of 550 ℃ should form.

Slightly different view of TG–DSC curves by thermal treatment of Ca–Mo–O tartrate gel precursor, presented in Fig. 2, is shown. In this case overall weight loss of about 74 % of analyzed specimen to 775 °C temperature has occurred. The thermal decomposition processes of the Ca–Mo–O tartrate system likewise in previous case also into eight periods have divided.
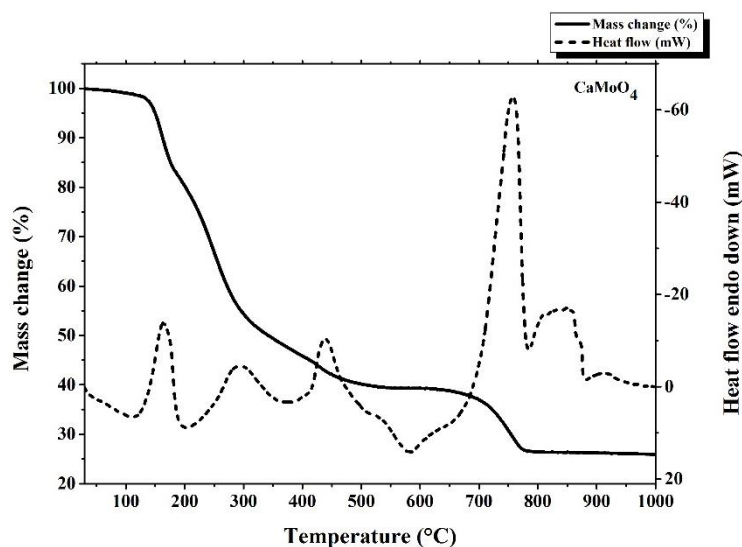

Fig. 2 Combined TG–DSC curves of the Ca–Mo–O tartrate gel precursor in flowing air

The first weight loss of about 2 % in the TG curve takes from 60 °C to 130 °C temperatures and is related with the removal of surface absorbed water from the gel and/or water from the coordination sphere of the metal complexes. An endothermic peak of heat flow of 403 mJ and $\Delta H = 40$ J/g on the DSC curve corresponds to the first period of weight loss. The initial thermal dissociation of tartaric acid in the precursor gel or the decomposition reaction of mixed-metal nitrate and ammonium salts that were formed during the sol-gel processing start from 130 – 140 °C temperature, respectively. This weight loss of about 9 % follows the exothermic transformations with a peak width of about 2247 mJ ($\Delta H = -217$ J/g). The third weight loss of about 14 % from 210 °C temperature, in this case, to the final decomposition of the excess of tartaric acid in the sample could be attributed. The exothermic peak of about 2238 mJ ($\Delta H = -215.9$ J/g) from 240 °C to 350 °C temperature corresponds with the third period of weight loss. Next to that, the burning of the small amount of elemental carbon of about 1 % that has formed during the partial decomposition and intermolecular rearrangement of tartaric acid has been observed. Comparatively to the low weight loss in this stage a strong exothermic peak of about 1898 mJ ($\Delta H = -183$ J/g)

10

was measured. The fifth stage on the DCS curve from 520 °C to 670 °C temperature with no weight changes in the analyzed sample characterized by endothermic effect of about 1996 mJ ($\Delta H = 192.5$ J/g) to the crystallization of $CaMoO_4$ phase is related. Finally, the last weight loss of about 12 % from 700 °C to 780 °C temperature with the decomposition of carbonates that formed during the partial oxidation of metal tartrates in the Ca–Mo–O gel precursor have occurred. A strong exothermic peak of about 8225 mJ ($\Delta H = -793$ J/g) in this period corresponds to the decomposition process of hydrocarbons with the evaporating of CO_2 and H_2O gases. As seen from the DSC curve in the 780 – 880 °C temperature range another broad exothermic band of about 2450 mJ ($\Delta H = -236.4$ J/g) is observed. This negative heat effect is closely related with the earlier exothermic process and the further crystallization of $CaMoO_4$ phase in the same matter of time. In conclusion, it should be noted that the final decomposition of Ca–Mo–O tartrate gel precursor occurs at the temperature of 780 °C. However, the crystallization process, likewise as was mentioned in previous case, also starts at relatively low temperature of 550 °C.

The combined TG–DSC curves of Sr–Mo–O tartrate gel precursor in Fig. 3 are displayed. The decomposition of all volatile parts in Sr–Mo–O sample to 600 °C temperature has occurred.
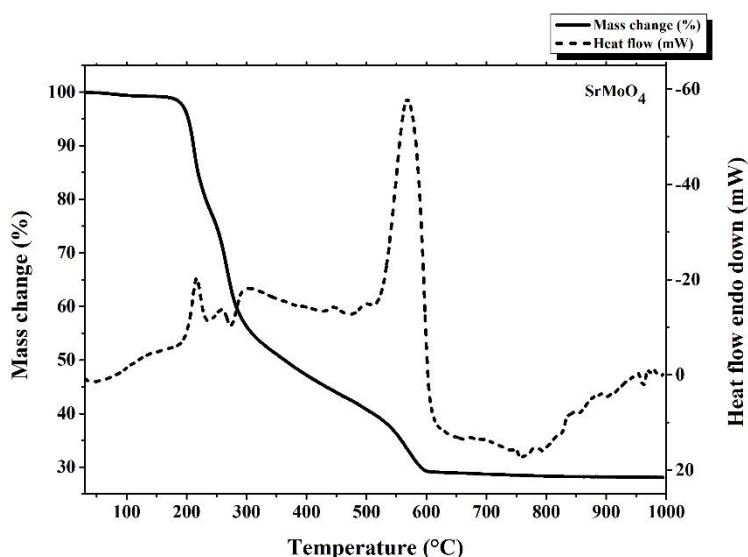

Fig. 3 Combined TG–DSC curves of the Sr–Mo–O tartrate gel precursor in flowing air

The general behavior of TG–DSC curves of Sr–Mo–O gel in six periods has divided. In the first period the evaporation of adsorbed water molecules with a weight loss of about 0.5 % and an endothermic peak of about 426 mJ ($\Delta H = 72$ J/g) to 140 °C temperature was

11

occurred. After that in the second period with a weight loss of about 14 % from 150 °C to 240 °C temperature the decomposition of tartaric acid and either ammonium or nitrate ions was started. The decomposition of above mentioned compounds to CO_2 and NO_x gases by the exothermic peak of about 551 mJ (ΔH = –94 J/g) was confirmed. Next to that in the third and fourth periods from 245 °C to 500 °C temperatures the further decomposition of metal tartrates with weight loss of about 9 % overlaps with the intermolecular rearrangement of residual products of tartaric acid. This conclusion by well-defined exothermic peak of about 166 mJ (ΔH = –28 J/g) from 255 °C to 270 °C temperatures and by overlapped both exothermic and endothermic processes in the range of 280 – 450 °C temperature has suggested. Further increasing of temperature from 450 °C to 505 °C leads to the start of crystallization of the final $SrMoO_4$ phase that confirmed a broad endothermic peak of about 175 mJ (ΔH = 30 J/g) in the DSC curve. Finally, the weight loss of about 7 % from 520 °C to 600 °C temperature with an exothermic peak of about 8038 mJ (ΔH = –1366.5 J/g) by combusting of residual organic compounds and as-formed inorganic carbon has been characterized. In the last six period of thermal investigation of Sr–Mo–O gel precursor, the TG curve has remained constant. However, in the DSC curve a broad endothermic band related with the crystallization process near to the 1000 °C temperature has been observed. In conclusion, TG/DSC analysis of Sr–Mo–O tartrate gel precursor showed that pure single-phase crystalline $SrMoO_4$ compound at temperature of 600 °C should form. However, the crystallization process of $SrMoO_4$ starts under 500 °C temperature that clearly the results from DSC curve.

The last combined TG–DSC curves of Ba–Mo–O tartrate gel precursor in Fig. 4 have shown. The character of weight loss in the TG curve is similar comparing with previous cases when the weight of Ba–Mo–O tartrate gel precursor over 600 °C temperature remains constant. However, the general views of TG–DSC curves of the Ba–Mo–O sample and conclusions that have made from this thermal analysis are significantly different in comparing with the three cases presented before. The TG–DSC analysis of Ba–Mo–O tartrate gel precursor was divided into five weight loss periods. The first exothermal peak of about 977 mJ (ΔH = –219 J/g) from 60 °C to 165 °C temperature indicates that the first weight loss of about 5 % in the sample is close related with the thermal decomposition of ammonium and nitrate ions to the N_2 and NO_x gaseous products. This exothermal process overcomes the endothermic peak of the evaporation of water molecules from the gel that

was not well expressed in the previous cases. By the further increase of temperature from 170 °C to 300 oC, the typical decomposition process of tartaric acid with weight loss of about 60 % has been observed. A strong exothermic behavior of about 8383 mJ (ΔH = –1878 J/g) in the DSC curve was expressed. After that in the range of 300 – 500 °C temperature further decomposition and the rearrangement of organic parts in the gel precursor with weight loss of about 10 % has occurred. Finally, from the 500 °C temperature the combustion of residual carbon with weight loss of about 10 % in the sample has started. In addition, it is interesting to note that this burning process in at least to weight losses of about 2.5 and 1 % has been divided. In the DSC curve two exothermic peaks of about 2486 mJ (ΔH = –557 J/g) and 233 (ΔH = –52 J/g) mJ have been shown. By the further increase of temperature, the weight in the TG curve remains constant. The endothermic character of the DSC curve lets us conclude that in this range of temperature the crystallization of BaMoO$_4$ has dominated.
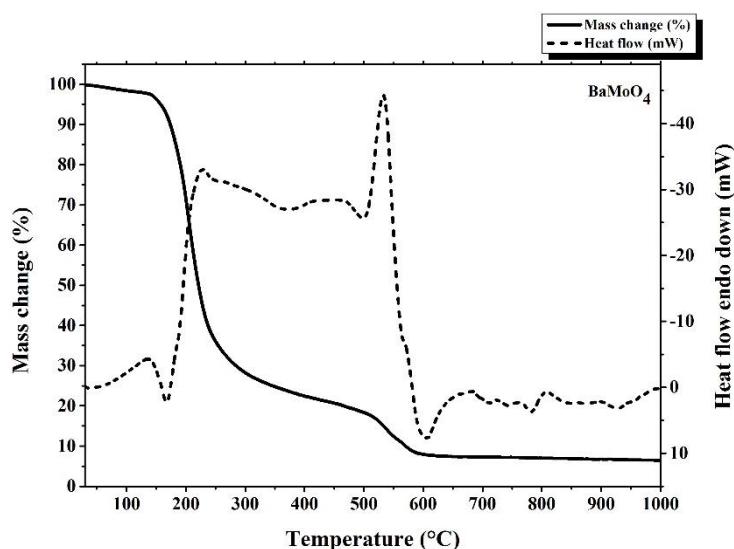

Fig. 4 Combined TG–DSC curves of the Ba–Mo–O tartrate gel precursor in flowing air

In conclusion, the thermal decomposition of above described fourth gel precursors occurred in different ways depending on the alkali earth metal in the starting materials.

X-ray diffraction

The X-ray diffraction (XRD) data were collected at room temperature with Cu–Kα_1 radiation and a scan range from 10 to 70 degrees for 2θ. XRD patterns of Mg–Mo–O

tartrate gel annealed at different temperatures shown in the top three panels in Fig. 5, are matched with that of standard ICSD card of $MgMoO_4$ shown in the bottom panel. In addition, XRD results indicated that even at 500 °C crystalline monoclinic $MgMoO_4$ phase has formed. By increase of temperature to 1000 °C the characteristic peaks of investigated samples became sharper and no new crystal phases have appeared. These results are in good agreement with the well-known tendency that at higher annealing temperatures, the crystallinity of mixed metal oxides increases. These obtained results are consistent with the conclusions made from TG–DSC analysis of Mg–Mo–O tartrate gel precursor that showed well-expressed ending temperature of weight loss and suggested possible crystallization point of final material with initial composition of $MgMoO_4$ phase.
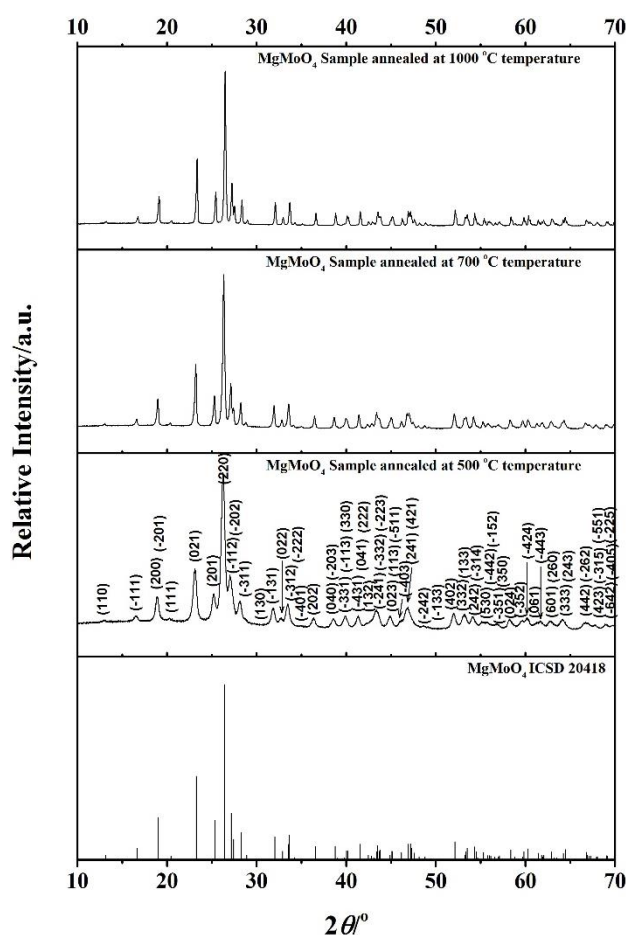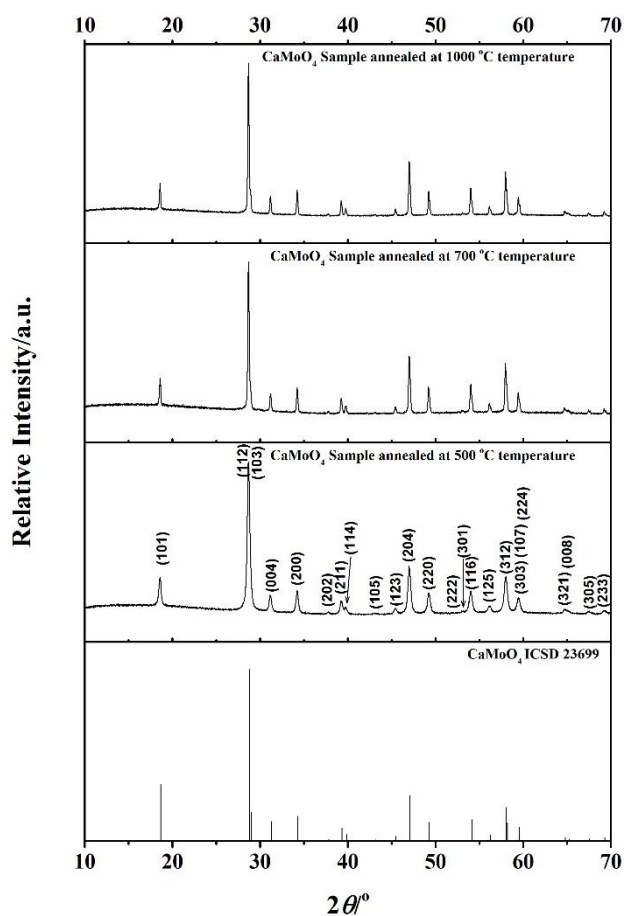

Fig. 5 Standard ICSD card of $MgMoO_4$ and XRD patterns of the Mg–Mo–O tartrate gel precursor annealed at 500, 700, and 1,000 °C temperatures

Figure 6 exhibits powder X-ray diffraction (XRD) patterns of the $CaMoO_4$ samples obtained by sintering the dried Ca–Mo–O tartrate gel precursor for 5 h at 500, 700 and 1000 °C temperatures in air atmosphere at ambient pressure. Despite the fact that

14

according to the TG–DSC analysis overall weight loss of about 74 % of analyzed Ca–Mo–O gel precursor to 775 ⁰C temperature has occurred, the crystallization of Powellite structured $CaMoO_4$ phase only above 500 ⁰C in XRD pattern (Fig. 6) has been identified. By increasing of temperature from 500 ⁰C to 700 ⁰C and 1000 ⁰C the characteristic peaks of $CaMoO_4$ crystal phase became sharper and better indexed that denote the growing of crystallite size in the final material. In addition, according to the XRD and TG–DSC results of investigated Ca–Mo–O precursor and sintered $CaMoO_4$ compound could be confirmed the conclusion that the weight loss above 700 ⁰C temperature because of the combustion of either hydrocarbons and/or elemental carbon has occurred.

Fig. 6 Standard ICSD card of $CaMoO_4$ and XRD patterns of the Ca–Mo–O tartrate gel precursor annealed at 500, 700, and 1,000 ⁰C temperatures

Moreover, according to the consistent results of XRD patterns of both investigated systems to explain the marked differences between TG–DSC curves an additional investigation is required.

15

Fig. 7 exhibits the X-ray diffraction (XRD) patterns of the $CaMoO_4$:1%Eu^{3+} powders obtained by sintering the dried gels for 5 h at 650, 700, 750 and 800 °C temperatures. As seen, the calcination of Ca(Eu)–Mo–O tartrate precursor gel powders at different temperatures produces a fully crystalline $CaMoO_4$ phase and no characteristic peaks due to the side crystalline Eu_2O_3 or Eu_2MoO_6 phases were observed. When the dried gels were calcined at 650, 700, 750 and 800 °C temperatures only the tetragonal $CaMoO_4$ phase appeared, which corresponds to ICSD file number 62219. These results clearly indicate that the crystallization of the $CaMoO_4$ phase is entirely complete at the relatively low temperature of 650 °C and this is in a good agreement with the TG–DSC results. However, some low intense impurity peaks in the XRD pattern of the powders calcined at 700 °C (see Fig.7 middle panel) could be indexed as a MoO_3 crystalline phase. In addition, no characteristic peaks attributable to the CaO crystal phase were identified. On the other hand, by further increasing sintering time and temperature the diffraction lines from impurity phase disappeared, and the XRD patterns of the samples annealed at 750 °C and 800 °C temperatures showed only monophasic crystalline $CaMoO_4$ (Fig. 7).
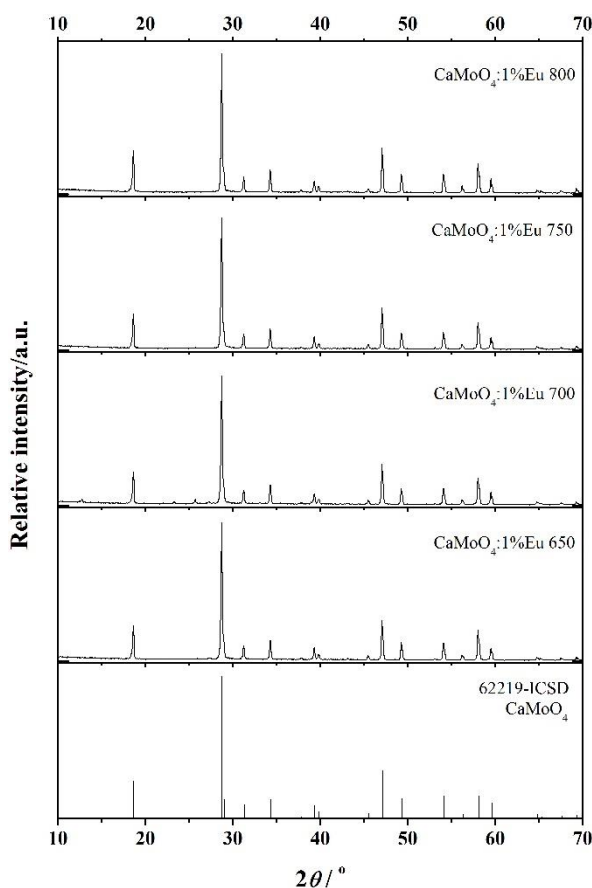

Fig. 7 Standard ICSD card of $CaMoO_4$ and XRD patterns of the Ca(Eu)–Mo–O tartrate gel precursor annealed at 650, 700, 750 and 800 °C temperatures

16

XRD patterns of Sr–Mo–O tartrate gel precursor annealed at 500, 700 and 1000 °C temperatures in Fig. 8 are shown. In this case, all used annealing temperatures are suitable for preparation of single-phase crystalline $SrMoO_4$ compound. Moreover, these XRD data of sintered Sr–Mo–O tartrate system are in a good agreement with the with the TG–DSC results presented in Fig. 3.
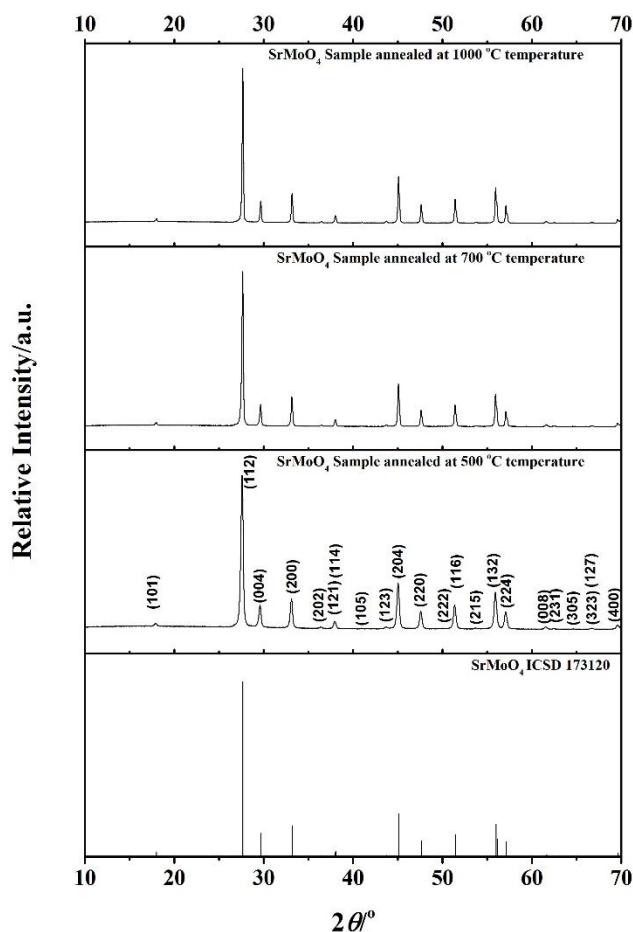

Fig. 8 Standard ICSD card of $SrMoO_4$ and XRD patterns of the Sr–Mo–O tartrate gel precursor annealed at 500, 700, and 1,000 °C temperatures

Slightly different results compared with previous cases after annealing of Ba–Mo–O tartrate gel precursor at 500, 700 and 1000 °C temperatures have obtained. Corresponding XRD patterns of this system in Fig. 9 are displayed.

For Ba–Mo–O tartrate sample annealed at 500 °C temperature, an extra XRD peaks at about 18.92°, 24.27°, 26.89°, 28.74° and 30.94° appeared, which belongs to monoclinic $BaMo_3O_{10}$ crystal phase (ICSD 50274) and compose 13.75 % as side phase in tetragonal crystal structure (ICSD 56109) displayed in a bottom panel (Fig. 9). By further increasing of annealing temperature to 700 °C the impurity peaks of monoclinic $BaMoO_4$ crystal

phase disappeared and only characteristic plane-structured reflections of tetragonal phase have dominated.
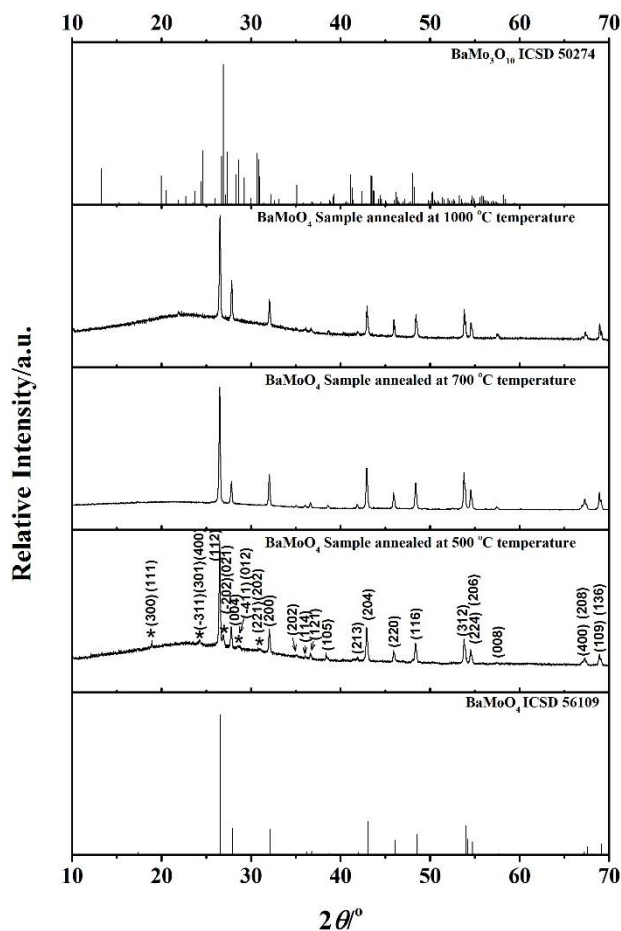

Fig. 9 Standard ICSD card of $BaMoO_4$ and XRD patterns of the Ba–Mo–O tartrate gel precursor annealed at 500, 700, and 1,000 $^{\circ}$C temperatures

Finally, the XRD pattern, displayed in next-to-last panel, shows the possible rearrangement of characteristic planes in tetragonal $BaMoO_4$ crystal phase by increasing of temperature to 1000 $^{\circ}$C. This conclusion have confirmed by the strong expressed endothermic signal in the DSC curve above 700 $^{\circ}$C, displayed in Fig. 4.

In summary, the XRD data of all investigated samples have revealed that using aqueous sol-gel processing at relatively low temperature of 500 $^{\circ}$C is possible to synthesize pure $MgMoO_4$, $CaMoO_4$ and $SrMoO_4$ crystal phases. Meanwhile, XRD patterns of the Ba–Mo–O tartrate gel precursor annealed at 500 $^{\circ}$C temperature the characteristic peaks that attributed to the monoclinic and tetragonal crystal phases of $BaMoO_4$ are observed. By increase of the annealing temperature to 700 $^{\circ}$C only tetragonal crystal structure of $BaMoO_4$ has found, as is presented in Fig. 9.

18

SEM micrographs

The surface morphology of $MgMoO_4$, $CaMoO_4$, $SrMoO_4$ and $BaMoO_4$ compounds prepared by aqueous sol-gel synthesis method and annealed at 700 and 1000 °C temperatures by scanning electron microscopy (SEM) was investigated. The representative SEM micrographs of $MgMoO_4$ sample are shown in Fig. 10 (a) and (b). The surface of the Mg–Mo–O tartrate gel precursor annealed at 700 °C temperature consists of the porous irregular particles of size from 500 nm to 3 μm. With further increasing of annealing temperature to 1000 °C the spherical crystalline particles in size of about 1 – 5 μm have estimated. These obtained results are in a good agreement with the broad endothermic band of about 6603 mJ in the stage of temperature from 800 to 1000 °C presented in DSC curve that characterize the crystallization and agglomeration processes of final crystalline material.

Slightly different results from SEM micrographs, presented in Fig. 6 (c) and (d), by combustion of Ca–Mo–O tartrate gel precursor were obtained. Figure 10 (c) shows SEM image of Ca-Mo-O sample sintered at 700 °C. In this case, the growing of homogenous spherical grains with an average diameter of about 200 – 300 nm are observed. Thereafter, the annealing temperature of 1000 °C leads to the formation of the crystals with well-expressed spherical shapes and edges that size varies from 1 to 5 μm.

Interesting results by combustion of Sr–Mo–O tartrate gel precursor from SEM micrographs in Fig. 10 (e) and (f) were observed. The homogeneous spherical grains of $SrMoO_4$ with an average diameter of about 500 nm have formed when the synthesis at 700 °C was carried out (Fig. 10 (e)). By increasing of annealing temperature to 1000 °C (Fig. 10 (f)) the surface of $SrMoO_4$ sample consists of close-packed spherical crystals with well-defined edges of size from 2 to 10 μm.

The tendency in changing of the surface morphology by combustion of the Ba–Mo–O tartrate gel precursor (Fig. 10 (g) and (h)) followed in the similar manner as was shown in previous cases. With increasing of sintering temperature to 700 °C leads to the agglomeration of close-packed spherical crystals with well-defined edges in size up to 20 μm that are surrounded by irregular crystals of size less than 5 μm. Figure 10 (h) shows the formation of crystals that form irregular agglomerates in size from 5 to 50 μm.
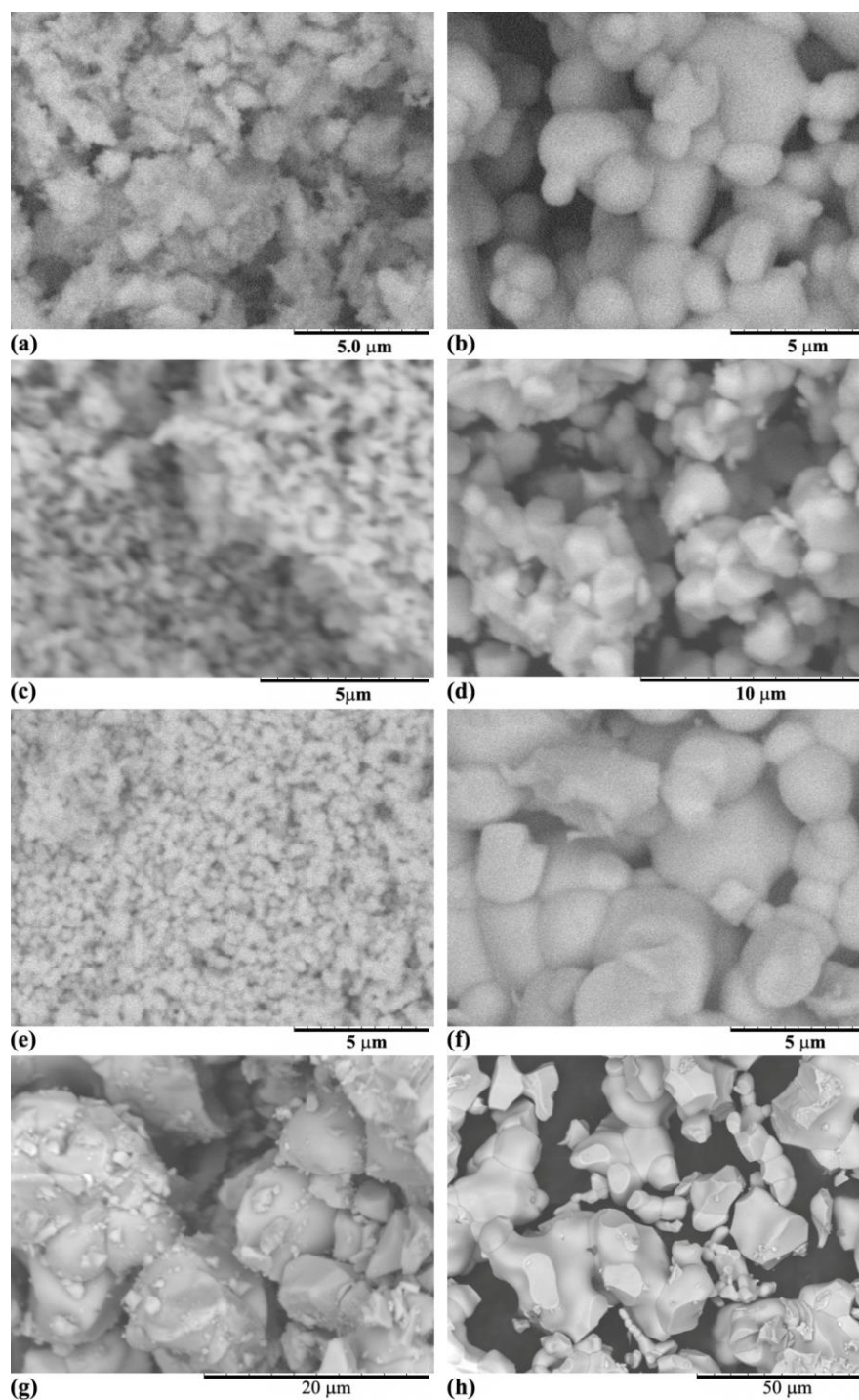
Fig. 10 SEM micrographs of Mg–Mo–O (a 700 ºC, b 1,000 ºC), Ca–Mo–O (c 700 ºC, d 1,000 ºC), Sr–Mo–O (e 700 ºC, f 1,000 ºC), and Ba–Mo–O (g 700 ºC, h 1,000 ºC) tartrate gel precursors annealed at different temperatures

In conclusion, it is clear that the surface morphology of investigated samples has significantly affected by both sintering temperature and nature of alkaline earth element. Summarizing results obtained from TG–DSC, XRD and SEM measurements can be concluded that aqueous sol-gel synthesis method is a suitable technique for the preparation

20

of single-phase $MgMoO_4$, $CaMoO_4$, $SrMoO_4$ and $BaMoO_4$ compounds at relatively low temperature of 500 °C. Moreover, according to the SEM results the formation of spherical crystals with well-expressed planes and edges have started up to 700 °C in $MgMoO_4$, $CaMoO_4$ and $SrMoO_4$ cases and below 700 °C in $BaMoO_4$ case, that are close related with the relative low melting point of barium molybdate crystal phase.

The SEM micrographs of $CaMoO_4$:xEu^{3+} samples prepared by the aqueous sol-gel method at 650, 700, 750 and 800 °C are shown in Figs. 15 – 20. The SEM results clearly indicate that all products consist of micrometer and sub-micrometer differently shaped particles with narrow crystal size distribution. The homogeneous spherical grains of $CaMoO_4$:1%Eu^{3+} with an average diameter of about 1 μm – 5 μm have formed when the synthesis was carried out at 650 °C (Fig. 11).
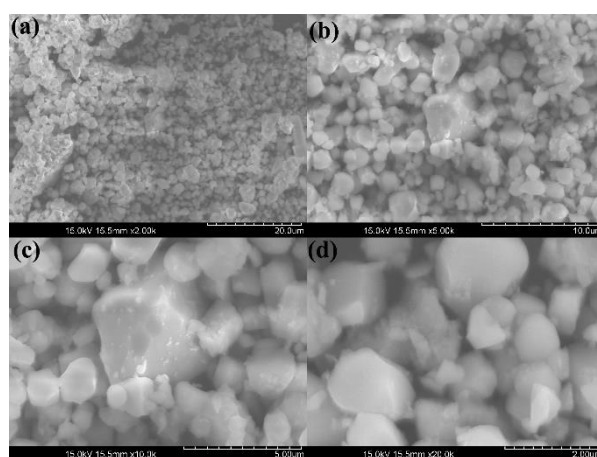

Fig. 11 SEM micrographs of 1 % Eu^{3+} ions doped $CaMoO_4$ sample synthesized at 650 °C in air atmosphere

As seen from micrographs at higher magnification (Fig. 11, c and d), the surface morphology of synthesized samples exhibits homogeneous packing of the micrograins where the larger particles (about 5 μm) are surrounded with smaller grains of about 1 μm diameter. However, the SEM image of $CaMoO_4$:6 %Eu^{3+} compound (Fig. 12, a) reveals the formation of plate-like larger crystals in size of about 15 μm – 20 μm.

These crystallites co-exist in close packing with spherical particles of size less than 2 μm (Fig, 12, b, c and d), indicating that the concentration of dopant has a small effect on the morphological features of the molybdate samples annealed at the 650 °C.
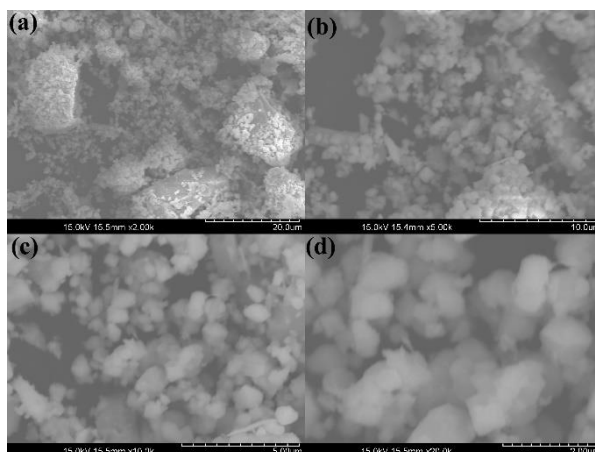
Fig. 12 SEM micrographs of 6 % Eu^{3+} ions doped $CaMoO_4$ sample synthesized at 650 °C air atmosphere
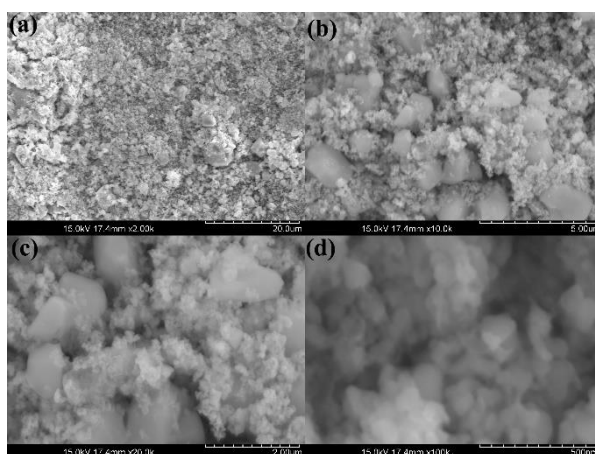

Fig. 13 SEM micrographs of 1 % Eu^{3+} ions doped $CaMoO_4$ sample synthesized at 700 °C in air atmosphere

As shown in Fig. 13, a – d, with increasing sintering temperature up to 700 °C two types of grains have formed. The smaller spherical particles, which are less than 200 nm size, tend to aggregate by many small crystal grains. Meanwhile, the larger grains form individual crystals rather than aggregate with each other. This observation could explain the impurity phase of MoO_3 in XRD pattern of the $CaMoO_4$:1%Eu^{3+} sample prepared at 700 °C for 5 h in air atmosphere.

With further increasing the temperature up to 750 °C, the particles tend to aggregate strongly showing good connectivity between grains (Fig. 14).
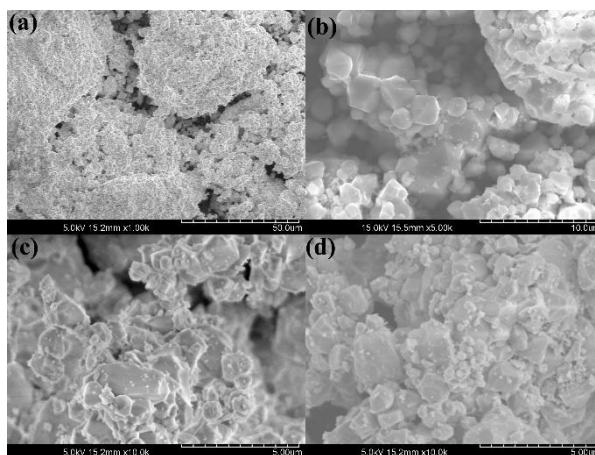
Fig. 14 SEM micrographs of 1% Eu^{3+} ions doped CaMoO$_4$ sample synthesized at 750 °C in air atmosphere.

Less than 3 μm plate-like crystals with narrow size distribution CaMoO$_4$:1% Eu^{3+} sample have formed at this temperature. Fig. 15 shows the SEM micrograph of the CaMoO$_4$:1%Eu^{3+} sample synthesized at 800 °C for 5 h in air atmosphere.
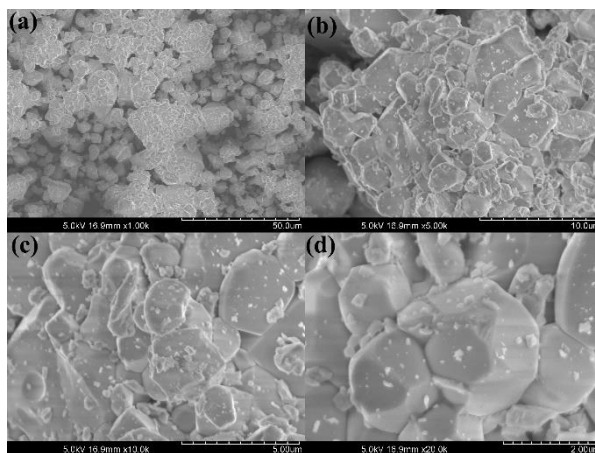

Fig. 15 SEM micrographs of 1% Eu^{3+} ions doped CaMoO$_4$ sample synthesized at 800 °C in air atmosphere.

However, the surface morphology of the CaMoO$_4$:1%Eu^{3+} powders synthesized at 800 °C for 5h are very similar to those prepared at 750 °C. The higher temperature produced just a bit larger crystals. Fig. 16 represents the SEM image of CaMoO$_4$:6%Eu^{3+} synthesized at 800 °C for 5 h in air atmosphere. Again, with increasing concentration of europium the larger crystallites of the ceramic material have formed.
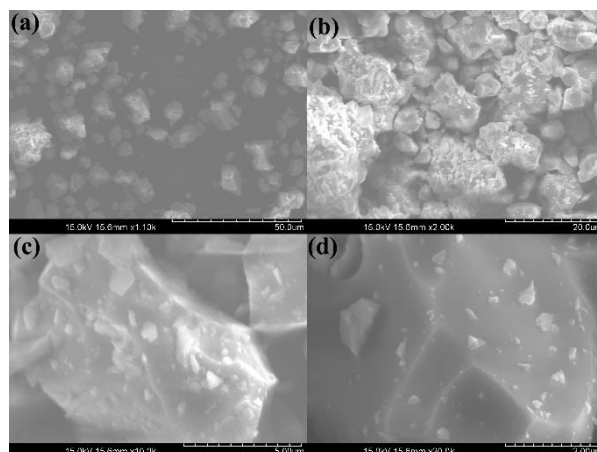
Fig. 16 SEM micrographs of 6 % Eu^{3+} ions doped $CaMoO_4$ sample synthesized at 800 °C in air atmosphere

The high-magnification SEM images (Fig. 16, c and d) revealed that synthesized products consist of different crystallites with diameter of 2 μm – 4 μm and length 5 μm – 7 μm. These SEM results of the $CaMoO_4$:x%Eu^{3+} samples annealed at different temperatures confirmed that the sintering temperature and the dopant concentration could strongly affect on the morphological features of final products.

FT-IR analysis

The infrared spectra of the synthesized $CaMoO_4$:xEu^{3+} samples annealed at 650 °C for 5 h are shown in Fig. 17. All FT-IR spectra of the $CaMoO_4$:xEu^{3+} specimens qualitatively are very similar regardless the concentration of europium in the material.
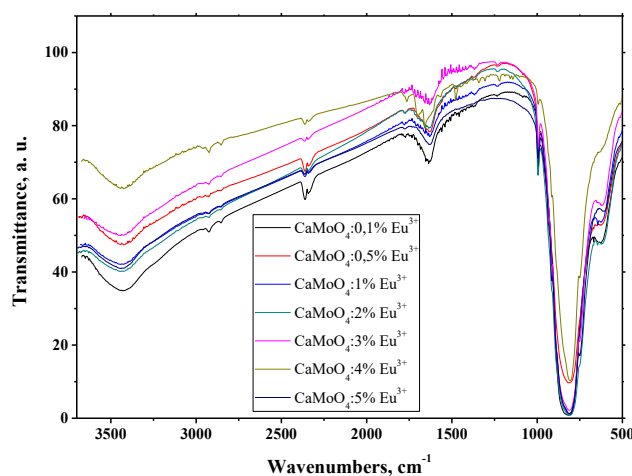

Fig. 17 FT–IR absorption spectra of $CaMoO_4$:xEu^{3+} samples.

The bands at 3454 cm^{-1} and 1631 cm^{-1} are assigned to O–H stretching vibration and H–O–H bending vibrations, respectively. These two bands are the characteristic vibrations of water from air, physically absorbed on the sample surface that is completely different from coordinated water in compound. A strong absorption band at around 910 cm^{-1} is related to O–Mo–O stretches of the MoO$_4$ tetrahedron. The AWO$_4$ type scheelite oxides having S$_4$ symmetry for the WO$_4^{2-}$ groups also show the main absorption bands in the region of 400–1000 cm^{-1}, centred around 911, 833 and 405 cm^{-1} corresponding to the ν1, ν3 and ν2 modes of the WO$_4^{2-}$ groups, respectively. It is also important to note, that the FT–IR spectra of Eu$_2$O$_3$ doped calcium molybdate samples calcined at 650 °C did not show any bands attributable to carbonates or residual organic species.

Reflection measurements

The optical properties of doped with europium CaMoO$_4$ ceramics synthesized using the nitrate-tartrate sol-gel technique were also investigated. UV-vis reflectance spectra of CaMoO$_4$:x%Eu^{3+} (x = 1, 2, 3, 4, 5 and 6) phosphor are shown in Figs. 18 – 20.

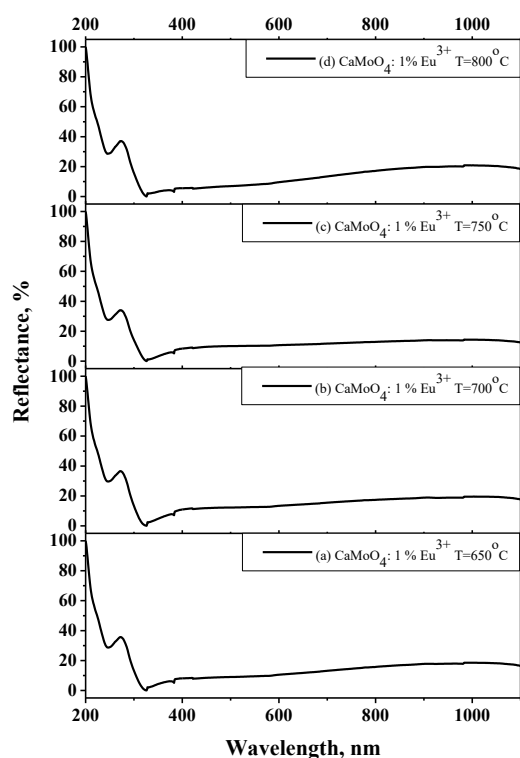**Fig. 18** UV–vis reflectance spectra of crystalline CaMoO$_4$ doped with 1 % Eu^{3+} ions and annealed at 650 °C (a), 700 °C (b), 750 °C (c) and 800 °C (d) temperatures

CaMoO$_4$ nano-crystals exhibited a very broad asymmetric reflection in the range of 180 nm – 300 nm, which is also observed in Fig. 18 of the CaMoO$_4$:1%Eu^{3+} samples annealed at 650 °C – 800 °C temperatures. Additionally, the reflectance spectra of all samples are very similar. The reflection bands of CaMoO$_4$:1%Eu^{3+} samples are located between 200 nm and 315 nm, corresponding to oxygen to molybdenum (O→Mo) ligand-to-metal charge transfer in the MoO$_4^{2-}$ group. As is shown in Fig. 19, the reflection bands at 362, 367, 377, 382, 385 nm and sharp peaks at 394, 465 nm could be attributed to the reflectance of Eu^{3+} ions in the CaMoO$_4$ host-lattice. Moreover, the sharp peak at 394.8 nm tends to increase (see Fig. 20) by increasing dopant concentration in CaMoO$_4$ host-lattice. However, the peak intensity of the CaMoO$_4$:x%Eu^{3+} samples annealed at 750 °C reached the maximum only with doping of 5 mol% of Eu^{3+} ions and further increasing of dopant concentration leads to the quenching of reflectance of obtained optical materials.
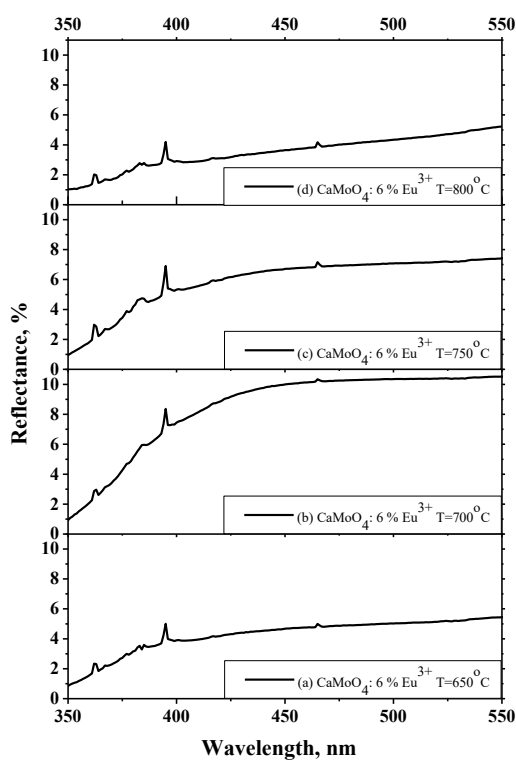
Fig. 19 UV–vis reflectance spectra of crystalline CaMoO$_4$ doped with 6 % Eu^{3+} ions and annealed at 650 °C (a), 700 °C (b), 750 °C (c) and 800 °C (d) temperatures

As can be seen from Fig. 19, the annealing temperature only little affects the optical properties of CaMoO$_4$ doped with 6% of Eu^{3+}. The maximum intensity of reflection peak at 394.8 nm of excitation light achieved in the sample synthesized at 750 °C temperature.
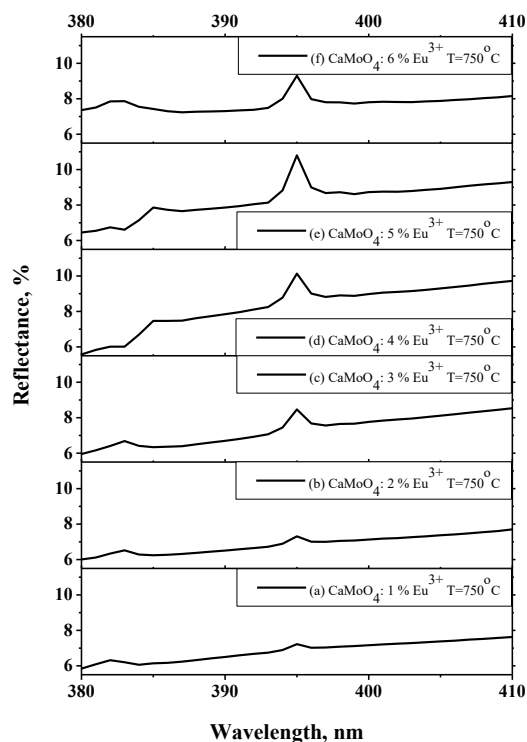
Fig. 20 UV–vis reflectance spectra of CaMoO$_4$:1%Eu^{3+} (a), CaMoO$_4$:2%Eu^{3+} (b), CaMoO$_4$:3%Eu^{3+} (c), CaMoO$_4$:4%Eu^{3+} (d) CaMoO$_4$:5%Eu^{3+} (e), CaMoO$_4$:6%Eu^{3+} (f) annealed at 750 °C

In conclusion, it should be noted that all synthesized CaMoO$_4$:xEu^{3+} samples were optically active compounds at shorter wavelengths (200–310 nm) that arises from MoO$_4^{2-}$ functional groups. Reflection peaks in 360–470 nm wavelength region are attributed to the Eu^{3+} characteristic excitations, which are significantly influenced by both annealing temperature and dopant concentration in CaMoO$_4$ lattice.

CONCLUSIONS

1. For the first time in our knowledge the aqueous tartaric acid-assisted sol-gel synthesis technique was successfully proposed for the preparation of M–Mo–O tartrate gel precursors and MMoO$_4$ ceramic materials (M=Mg, Ca, Sr and Ba) as well as europium oxide doped CaMoO$_4$ double oxide.

2. TG and DSC analysis of Mg–Mo–O, Ca–Mo–O, Sr–Mo–O and Ba–Mo–O tartrate gels clearly showed that the crystallization of final double oxides starts below 500

ºC. In the case of Mg–Mo–O, Sr–Mo–O and Ba–Mo–O tartrate precursors the combustion of volatile components and the burning of carbon residue occurs up to 600 ° C. Meanwhile, the decomposition of Ca–Mo–O tartrate gel and the final mass change determined up to 750 ºC.

3. Using X-ray diffraction (XRD), it has been observed that the characteristic peaks of $MgMoO_4$, $CaMoO_4$, $SrMoO_4$ and $BaMoO_4$ compounds are observed at temperatures between 500 ºC and 1000 ºC. Only in the case of $BaMoO_4$, at 500 ºC, the peaks of the low-intensity of $BaMo_3O_{10}$ were noticed, which disappears when the heating temperature is increased to 600 ºC.

4. The XRD results of Ca–Mo–Eu–O tartrate gel powders, which were annealed at 650, 700, 750 and 800 ºC, showed that the samples of $CaMoO_4:xEu^{3+}$ crystalize into tetragonal crystalline structure of $CaMoO_4$ compound. Besides, any characteristic peak of X-ray reflection for Eu_2O_3 or Eu_2MoO_6 compounds did not identified in the X-ray diffractograms. In addition, the small peaks of the MoO_3 compound were identified in $CaMoO_4$ sample at the temperature of 700 ° C, which disappear by the increase the annealing temperature up to 750 ° C and 800 ° C.

5. According to the scanning electron microscopy, the morphology of the surface of ceramic compounds depends really much from the nature of alkaline earth metal in M–Mo–O tartaric precursor. By increasing the annealing temperature the growth of spherical particles was observed. In the case of $MgMoO_4$, $CaMoO_4$ and $SrMoO_4$, above 700 ºC of temperature the particles of the spherical shape in size from about 200 nm to 3 μm were formed. Meanwhile, in the case of $BaMoO_4$, at the temperature of 700 °C the spherical particles in size from about 20 μm to 50 μm were determined. Such difference between separate samples is directly related to the lower melting point of barium molybdate comparing with other alkaline earth metal molybdates.

6. The SEM results of the morphology of the surface of europium doped calcium molybdate have clearly shown that the ion of the Eu^{3+} accelerates the growth of calcium molybdate crystals, which strongly affects the peculiarities of the morphology of the final two-component oxide surface.

7. The FT–IR spectra of Eu_2O_3 doped calcium molybdate samples annealed at 650 °C did not show any bands attributable to carbonates or residual organic species.

8. According to the UV–Vis spectra is clear that all synthesized $CaMoO_4:xEu^{3+}$ samples were optically active compounds at shorter wavelengths (200–310 nm) that arises from MoO_4^{2-} functional groups. Reflection peaks in 360–470 nm wavelength region are attributed to the Eu^{3+} characteristic excitations, which are significantly influenced by both annealing temperature and dopant concentration in $CaMoO_4$ lattice. The peak intensity of the $CaMoO_4:x\%Eu^{3+}$ samples annealed at 750 °C reached the maximum only with doping of 5 mol% of Eu^{3+} ions and further increasing of dopant concentration leads to the quenching of reflectance of obtained optical materials.

THE LIST OF ORIGINAL PUBLICATIONS BY THE AUTHOR

Articles in Journals

1. **G. Braziulis**, G. Janulevičius, R. Stankevičiutė, A. Žalga, Aqueous sol–gel synthesis and thermoanalytical study of the alkaline earth molybdate precursors, *Journal of Thermal Analysis and Calorimetry*, **118** (2014) 613–621.
2. **G. Braziulis**, R. Stankevičiutė, A. Žalga, Sol-gel derived europium doped $CaMoO_4:Eu^{3+}$ with complex microstructural and optical properties, *Materials Science (Medžiagotyra)*, **20** (1) (2014) 90-96.

Published Contributions to Academic Conferences

1. **G. Braziulis**, G. Gaidamavičienė, A. Žalga, Sol-gel synthesis, crystal structure, surface morphology, and FT-IR spectroscopical investigation of alkaline-earth metal molybdates. Open readings 2017: 60th International conference for students of physics and natural sciences, 14-17 March, Vilnius 2017, p.175.
2. **G. Braziulis**, G. Prievelytė, G. Janulevičius, A. Žalga, Tartaric acid-assisted sol-gel synthesis of various metal molybdates. Chemistry and chemical technology 2015: international conference of Lithuanian Chemical Society, dedicated to Professor Vitas Daukšas on his 80th birth anniversary, Vilnius, Lithuania, January 2 p. 70.

3. **G. Braziulis**, A. Žalga, Sol-gel synthesis of various metal molybdates. 58th Scientific Conference for Students of Physics and Natural Sciences "Open Readings 2015", March 24-27, 2015 Vilnius, Lithuania.

4. **G. Braziulis**, R. Raudonis, J. Raudonienė, A. Žalga. Aqueous tartaric acid assisted synthesis and thermoanalytical study of the magnesium and strontium molybdate-tungstate precursors. 11th European Symposium on thermal analysis and calorimetry, Espoo, Finland, 17-21 August 2014.

5. **G. Braziulis**, A. Žalga. Aqueous sol–gel synthesis of the Ba–Mo–O–(Eu^{3+}) powders. Advanced materials and technologies of the 16-th International conference-school, Palanga, Lithuania, 27-31 August, 2014.

6. **G. Braziulis**, A. Žalga. Aqueous sol–gel synthesis and FT-IR spectroscopical investigation of Eu^{3+} doped magnesium and strontium molybdates. Open readings 2014: 57th scientific conference for students of physics and natural sciences, 19-21 March, Vilnius 2014.

7. R. Gegevičius, **G. Braziulis**, A. Žalga. Šarminių žemių metalų molibdatų sintezė ir apibūdinimas. Studentų mokslinė praktika 2013.

8. **G. Braziulis**, G. Janulevicius, A. Zalga, Aqueous sol-gel synthesis and thermoanalytical study of the alkaline earth molybdate precursors. 2nd Central and Eastern European Conference on Thermal Analysis and Calorimetry, 27-30 August 2013, Lithuania.

9. **G. Braziulis**, A. Žalga, Mišraus bario molibdato-volframato sintezė ir charakterizavimas. Chemija ir cheminė technologija 2013: studentų mokslinės konferencijos pranešimų medžiaga, Vilnius 2013, gegužės 31 d.

Published Contributions to Academic Conferences Not Included in the Dissertation Thesis

1. G. Prievelytė, **G. Braziulis**, G. Janulevičius, A. Žalga, Phase transition in nanocrystalline Ca$_{1-x}$Sr$_x$MoO$_4$ synthesized by an aqueous sol-gel method. 58th Scientific Conference for Students of Physics and Natural Sciences "Open Readings 2015", March 24-27, 2015 Vilnius, Lithuania.

2. K. Marcinkevič, **G. Braziulis**, A. Žalga, Sol-gel synthesis and characterization of MgWO$_4$:x%Eu. 58th Scientific Conference for Students of Physics and Natural Sciences "Open Readings 2015", March 24-27, 2015 Vilnius, Lithuania.

CURRICULUM VITAE

Gediminas Braziulis

Education:

2004–2011 Bachelor Studies at Vilnius University – Bachelor Degree in Chemistry.

2011–2013 Master Studies at Vilnius University – Master Degree in Chemistry.

2013–2017 Postgraduate studies at the Department of Applied Chemistry, Faculty of Chemistry of Vilnius University.

Work experience:

2005 → Senior specialist at the Vilnius Gediminas Technical University Antanas Gustaitis' Aviation Institute.

2017 → Assistant at the Department of Mechatronics, Robotics and Digital Manufacturing, Faculty of Mechanics, Vilnius Gediminas Technical University.

ŠARMINIŲ ŽEMIŲ METALŲ MOLIBDATŲ SINTEZĖ IR TYRIMAS

SANTRAUKA

Per paskutinius kelis dešimtmečius, daugybė skirtingų sintezės technologijų buvo panaudota $MMoO_4$ (M = Mg, Ca, Sr ir Ba) savitos paviršiaus morfologijos kristalinių fazių gavimui. Ypatingai vadovaujantis šių dienų tendencijomis, kuomet tinkamas sintezės metodo pasirinkimas gali suteikti lemiamą pranašumą vystant mokslą ir pramonines technologijas. Todėl šio disertacinio darbo pagrindinis naujumas yra tiesiogiai susijęs su perspektyvaus ir retai publikuojamo vandeninio zolių-gelių sintezės metodo atmainos, kuomet geliacijos proceso metu naudojamas kompleksus su metalais sudaromas reagentas vyno rūgštis, vystymu šarminių žemių metalų molibdatų gamyboje.

Šiuo atveju, vandeniniu zolių-gelių sintezės metodu, kuomet zolių-gelių procese pirmą kartą panaudojus vyno rūgštį kaip kompleksus su metalais sudarantį reagentą, sėkmingai pavyko susintetinti vienfazius $MMoO_4$ pradinės molinės sudėties šarminių žemių metalų molibdatus bei homogeniškai legiruoti kalcio molibdatą $CaMoO_4:xEu^{3+}$ (kur x = 1, 2, 3, 4, 5, ir 6) skirtingomis europio oksido koncentracijomis. TG–DSC metodais ištyrus Mg–Mo–O, Ca–Mo–O, Sr–Mo–O ir Ba–Mo–O tartratinių gelių terminį skilimą, nustatyta, jog galutinių dvikomponenčių oksidų kristalizacija prasideda žemiau 500 ºC temperatūros. Galutinių organinių ir neorganinių Mg–Mo–O, Sr–Mo–O ir Ba–Mo–O tartratinių gelių lakių komponentų degimas įvyksta iki 600 ºC temperatūros. Tuo tarpu, Ca–Mo–O tartratinio gelio atveju, galutinis masės pokytis stebimas virš 750 ºC temperatūros. Panaudojus Rentgeno spindulių difrakcijos metodą (XRD) konstatuota, jog 500 ºC – 1000 ºC temperatūriniame intervale stebimos $MgMoO_4$, $CaMoO_4$, $SrMoO_4$ ir $BaMoO_4$ junginiams būdingos charakteringosios smailės. Tik $BaMoO_4$ dvikomponenčio oksido atveju, 500 ºC temperatūroje, išskiriamos žemo intensyvumo priemaišiniam $BaMo_3O_{10}$ junginiui būdingos smailės, kurios išnyksta padidinus kaitinimo temperatūrą iki 600 ºC. Iš Ca–Mo–Eu–O tartratinio gelio miltelių iškaitintų 650, 700, 750 ir 800 ºC temperatūrose XRD difraktogramų nustatyta, jog $CaMoO_4:xEu^{3+}$ pradinės molinės sudėties pavyzdžiai kritalinasi į tetragoninę $CaMoO_4$ dvikomponenčio oksido kristalinę struktūrą. Taip pat XRD rezultatuose nebuvo užfiksuoti jokie Eu_2O_3 ar Eu_2MoO_6 junginiams charakteringi Rentgeno spindulių atspindžiai. Be to, $CaMoO_4:1Eu^{3+}$ pradinės

molinės sudėties mėginio iškaitinto 700 ºC temperatūroje XRD difraktogramoje užfiksuotos MoO_3 junginiui būdingos smailės, kurios išnyksta padidinus kaitinimo temperatūrą iki 750 ºC ir 800 ºC. Pasitelkiant skenuojančiosios elektroninės mikroskopijos analizės metodą nustatyta, jog galutinių keramikinių junginių paviršiaus morfologija labiausiai priklauso nuo M–Mo–O tartratinių prekursorių sudeginimo temperatūros ir šarminio žemės metalo prigimties. Didinant kaitinimo temperatūrą stebimas sferinės formos dalelių augimas. $MgMoO_4$, $CaMoO_4$ ir $SrMoO_4$ pradinės molinės sudėties dvikomponenčių oksidų atveju virš 700 ºC temperatūros susiformuoja aiškios sferinės formos nuo 200 nm iki 3 µm dydžio dalelės. Tuo tarpu, $BaMoO_4$ dvikomponenčio oksido atveju, 700 ºC temperatūroje jau išskiriamos iki keliasdešimt mikrometrų dydžio sferinės formos atskiros dalelės. Šis skirtumas yra tiesiogiai susijęs su žemesne bario molibdato lydymosi temperatūra, lyginant su kitais šarminių žemių metalų molibdatais. Kalcio molibdato legiruoto skirtinga europio oksido koncentracija SEM paviršiaus morfologijos rezultatai aiškiai parodė, jog europio jonai labai paspartina kalcio molibdato kristalų augimą, o tai ženkliai įtakoja galutinio dvikomponenčio oksido paviršiaus morfologijos ypatumus. Iš FT–IR spektrų nustatyta, jog kalcio molibdato, legiruoto europio jonais ir iškaitinto 650 ºC temperatūroje, absorbcijos spektruose nėra aptinkama aborbcijos juostų charakteringų metalų karbonatams ar organinių junginių likučiams, kurie kaip priemaišiniai junginiai galėjo likti galutinėje keramikoje po kaitinimo aukštose temperatūrose. Remiantis UV–Vis analizės rezultatais akivaizdu, jog $CaMoO_4:xEu^{3+}$ pradinės molinės sudėties pavyzdžiuose vyksta krūvio pernaša iš deguonies į molibdeno atomus. Be to, didinant europio jonų koncentraciją sužadinimo smailės intensyvumas didėja, o pasiekus maksimalią koncentraciją – pradeda mažėti.